

CHAPTER IV

SPECTROMETRY

4.1 Fourier Transform Infrared Spectrometry

Infrared absorption spectra of fifty two Songea corundums representing all color varieties were obtained using Fourier Transform Infrared (FTIR) Spectrometer model NEXUS 470 FT-IR ESP (Figure 4.1) based at Department of General Science, Faculty of Science, Kasetsart University.



Figure 4.1 Fourier Transform Infrared (FTIR) Spectrometer (NEXUS 470 FT-IR ESP) belonging to Department of General Science, Kasetsart University.

4.2 Result

Representative spectra of each color variety are presented in Figures 4.2 to 4.6, respectively. In general, FTIR spectra observed from those corundum usually reveal similar absorption patterns within wave number range of $400\text{-}4000\text{ cm}^{-1}$. They contain peaks of CO_2 , probably caused by air and breath, at $2340\text{-}2360\text{ cm}^{-1}$, peaks of C-H stretching of hydrocarbon, may be coated along crack and surface, at $2840, 2920, 2950$ and 3051 cm^{-1} , peaks of H_2O likely from humidity at $3400\text{-}3900\text{ cm}^{-1}$ and peaks of structural O-H stretching at $3309, 3232$ and 3183 cm^{-1} (see Figures 4.2 to 4.6). Apart from common observation peaks, some red samples (Figure 4.2) show extensively declined curve within $3200\text{-}3700\text{ cm}^{-1}$ along with strongly absorption curve of C-H stretching. These samples were then examined again.

Consequently, many cracks were recognized; these cracks are suspected to contain iron stain, carbon polishing powder and humidity that may cause the mentioned curious curves. Besides they are possibly affected by diaspore ($\text{AlO}(\text{OH})$) in the stones. Hydrogen (H) in the environment may diffuse into crystal lattice and combine with oxygen (O) forming $\text{AlO}(\text{OH})$ structure that is invisible even observing under microscope but can be detected by FTIR at 3309 cm^{-1} absorption peak. The other significant absorption peaks are also observed in range of $400\text{-}1150\text{ cm}^{-1}$, particularly in red, blue and colorless varieties.

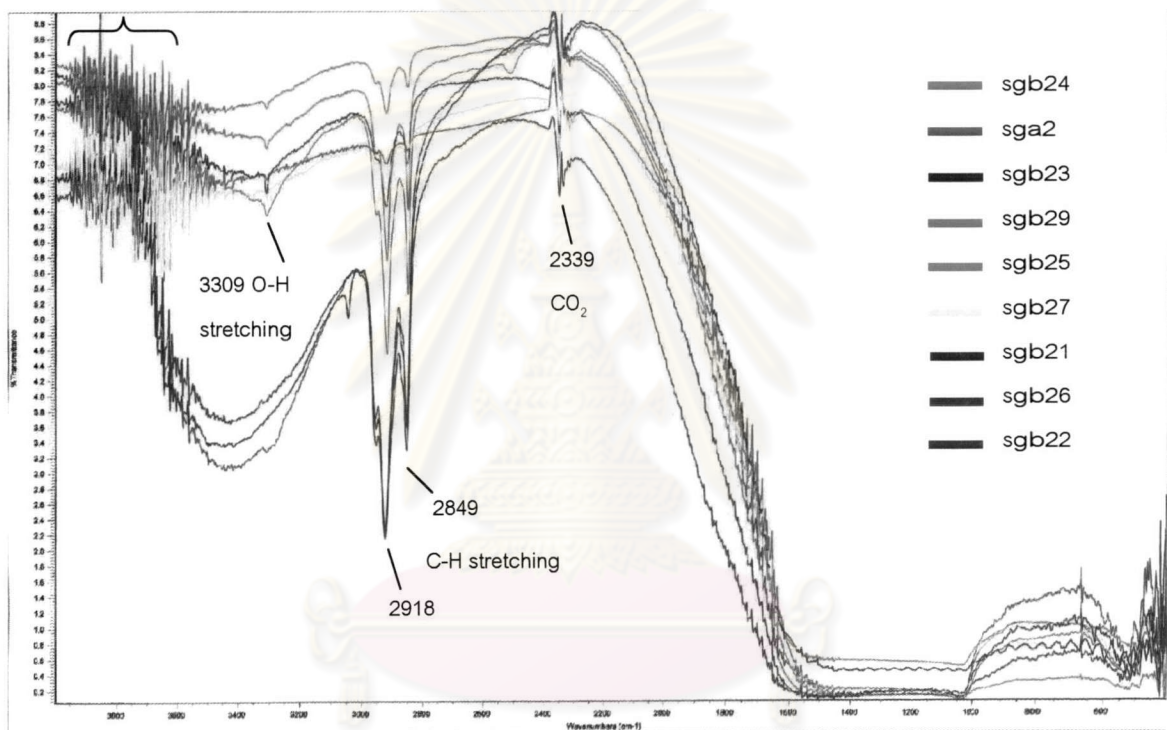


Figure 4.2 FTIR Spectra of red color variety.

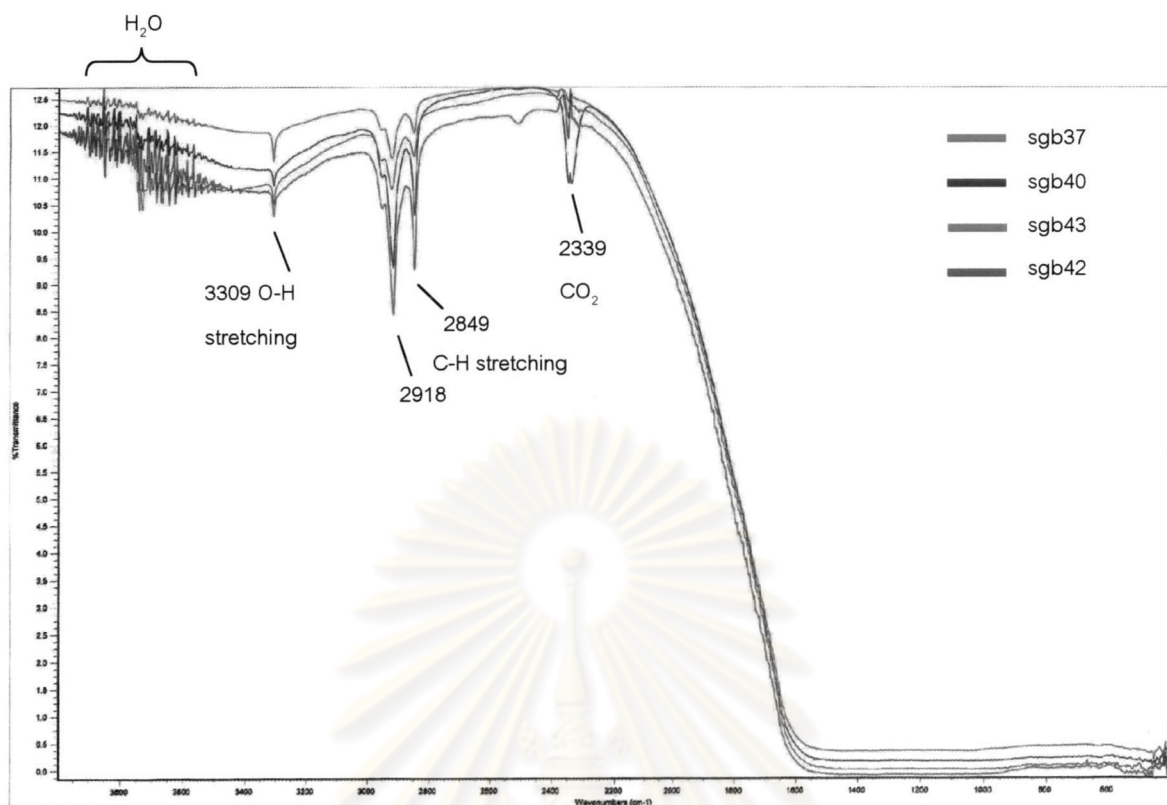


Figure 4.3 FTIR Spectra of purple color variety.

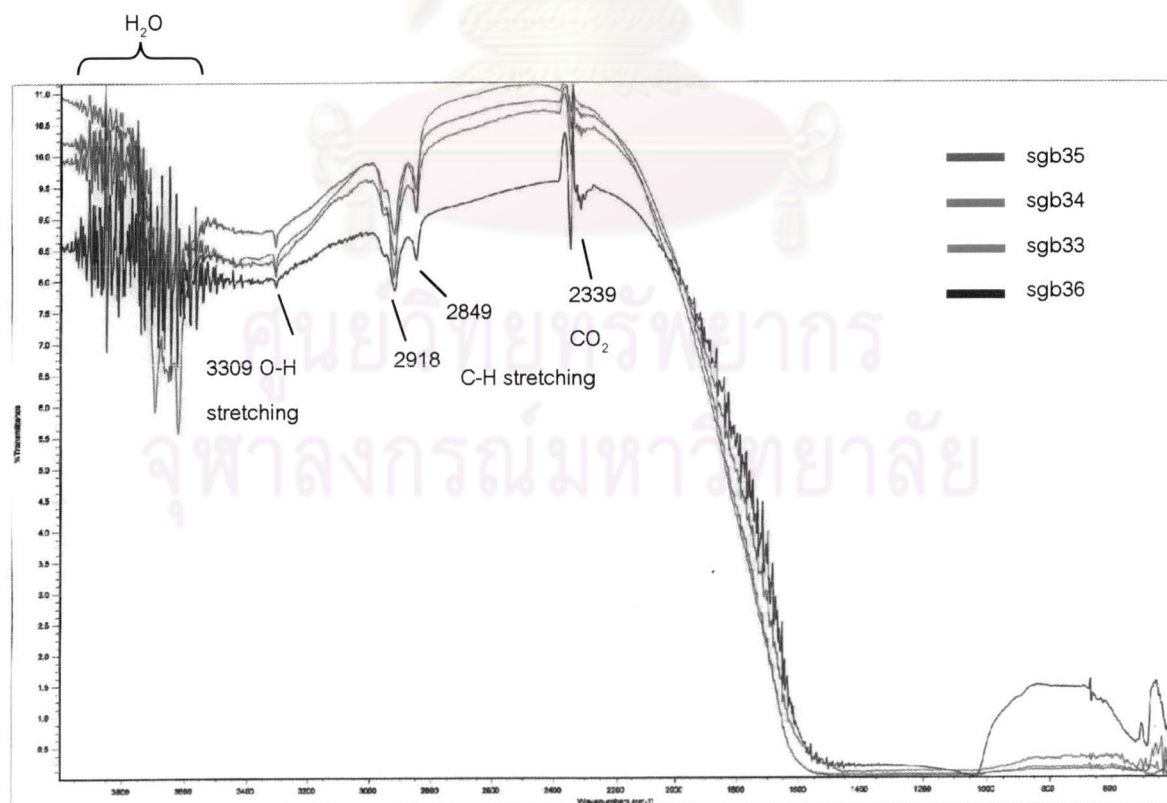


Figure 4.4 FTIR Spectra of blue color variety.

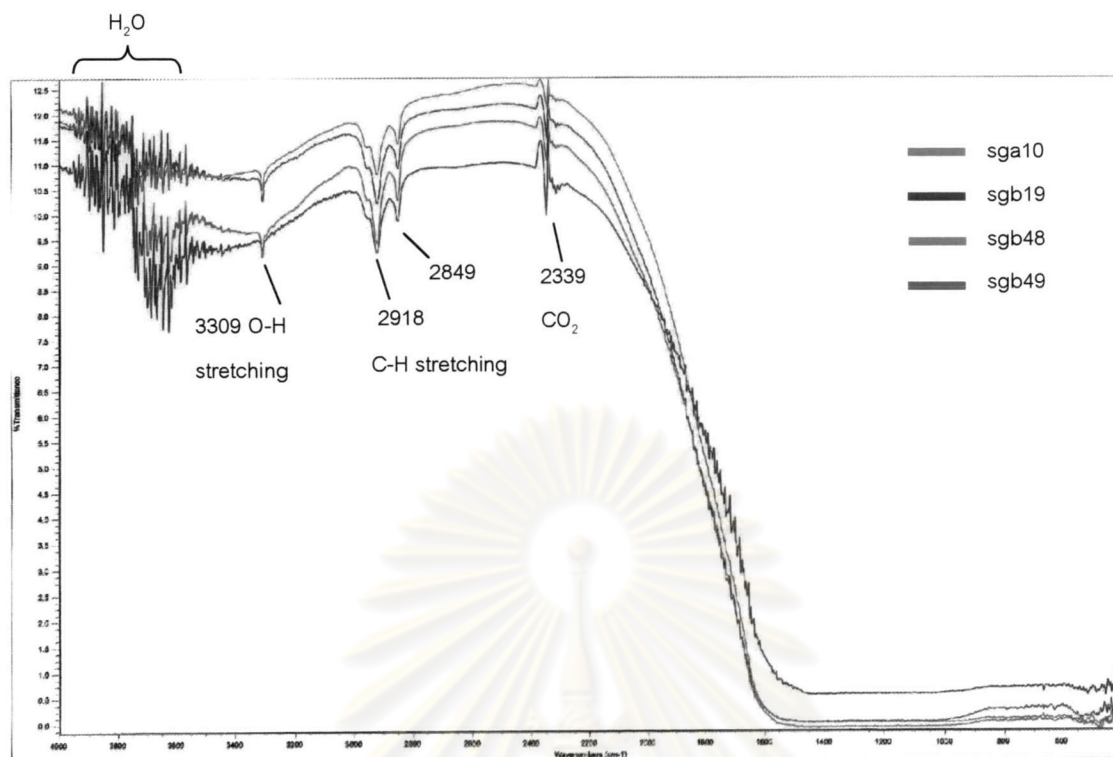


Figure 4.5 FTIR Spectra of yellow color variety.

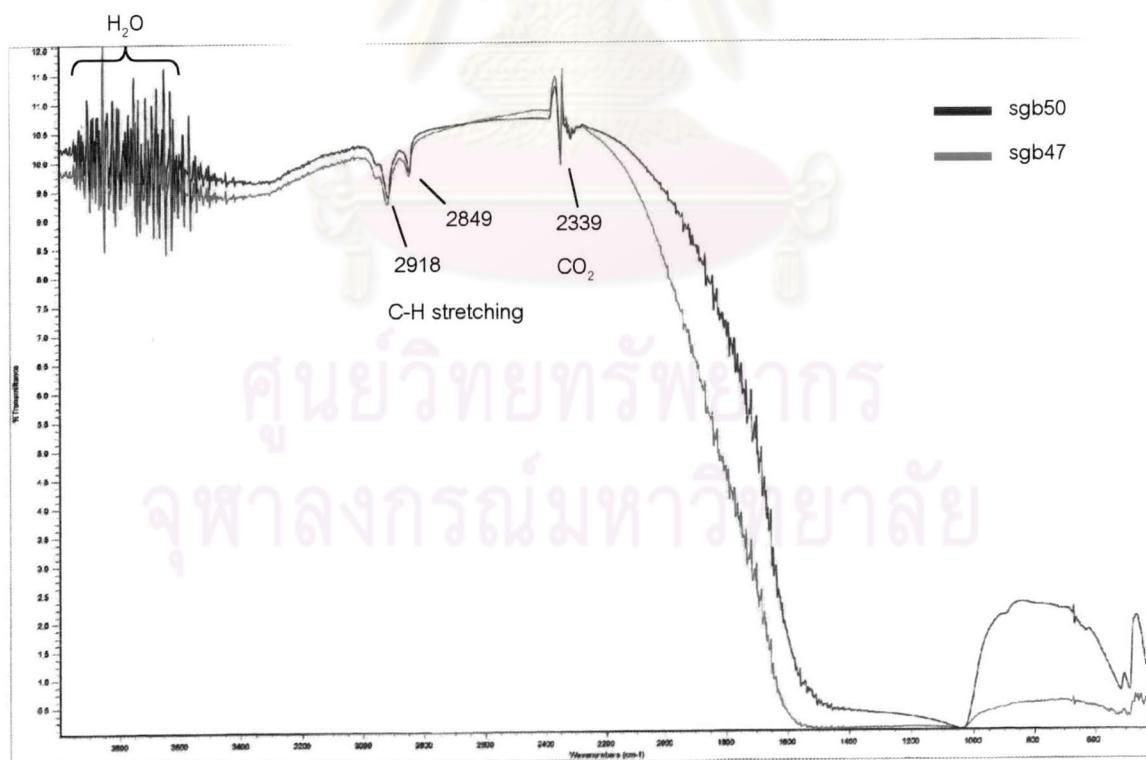


Figure 4.6 FTIR Spectra of colorless variety.

4.3 UV-VIS-NIR Spectrometry

From previous chapters, one of the most significant characteristics of Songea corundums is their multitude of variety of color. Consequently, they are sometimes called fancy corundum. The colors in corundum are mainly caused by Cr, Ti and Fe which are described below. The most crucial absorption spectra of corundum and other gemstones are usually investigated within wavelengths ranging between 200 and 1500 nm which are parts of ultraviolet (UV) (10-380 nm), full range of visible light (VIS) (380-780 nm) and parts of near infrared (NIR) (780-2500 nm). This kind of study is actually referred to UV-VIS-NIR spectrometry. For this research project, fifty two samples of unheated corundums were analyzed using HITACHI UV-VIS-NIR (model U-4001) spectrophotometer based at the Gem and Jewelry Institute of Thailand (GIT) (Figure 4.7).



Figure 4.7 UV-VIS-NIR spectrophotometer belonging to the Gem and Jewelry Institute of Thailand (GIT) was engaged for this research.

4.4 Result

Representative UV-VIS-NIR absorption patterns of 5 color varieties (i.e. red, purple, blue, yellow and colorless varieties) of Songea corundum are presented in Figures 4.8 to 4.20.

Red variety has various shades of red, red orange and orange that somehow yields slightly different UV-VIS-NIR absorption. The sample sgb29 which has red rim (R5/1) with orange core (O2/2) appears to have absorption peaks at 377 and 450 nm caused by $\text{Fe}^{3+}/\text{Fe}^{3+}$ ion pair, single Fe^{3+} ion peak at 388 nm and Cr^{3+} peaks at 412, 555 and 694 nm (Figure 4.8). The sample sgb21, that was given color codes as RO/OR6/3 respectively, yields a slightly different absorption pattern (Figure 4.9). This may be caused by details of color in each sample; the sample sgb21 seems to be more homogeneous in color while the sample sgb29 contain two different color areas (i.e. red and orange). Both absorption patterns however show peaks of Cr^{3+} at 412, 555 and 694 nm, and Fe^{3+} peak at 388 nm. The only difference appears at 377, 450 nm peaks of $\text{Fe}^{3+}/\text{Fe}^{3+}$ ion pairs which give yellow color was absent from the sample sgb21 (Figure 4.10).

The absorption pattern of orange corundum shows slightly different from those of the red variety. The absorption pattern of the sample sgb22 (Figure 4.10) shows absorption edges at somewhat higher wavelength, a Fe^{3+} peak at 388 nm, a peak of $\text{Fe}^{3+}/\text{Fe}^{3+}$ ion pair at 450 nm and peaks of Cr^{3+} at 555, 694 nm. The elevation of the absorption pattern toward the UV region is probably caused by the presence of yellow color center (Pisutha-Armond et al., 2004)

Purple variety is composed of purple, purple red, bluish purple, and etc which mostly show absorption patterns similar to those of the red variety. Samples in this variety however contain low Cr^{3+} with or without other color zones, such as yellow. Absorption patterns with little difference were observed within this variety. The sample sgb37 with color code drP5/3 has a resemble pattern (Figure 4.11) to that of the sample sgb29 of the red variety (Figure 4.8). It presents 377, 450 nm peaks of $\text{Fe}^{3+}/\text{Fe}^{3+}$ pairs, 388 nm peak of Fe^{3+} , 412, 555, 694 nm peaks of Cr^{3+} (Figure 4.11). However, Cr^{3+} peak at 412 nm is weak and sometimes absent (Figures 4.11 to 4.13). In addition, peak of $\text{Fe}^{2+}/\text{Ti}^{4+}$ at 565 nm become weak and broader, this may be caused by appearance of another $\text{Fe}^{2+}/\text{Ti}^{4+}$ IVCT peak at 588 nm (Figure 4.13). Absorption patterns of violet blue and blue samples (Figures 4.14 and 4.15)

are not quite different. The sample sgb31 (Figure 4.14), showing violet blue rim with yellow core, can provide representative characteristic of this color variety. Absorption peaks at 377, 450 nm caused by $\text{Fe}^{3+}/\text{Fe}^{3+}$ pairs are always present along with 388 nm peak of Fe^{3+} and 565 nm peak of $\text{Fe}^{2+}/\text{Ti}^{4+}$ IVCT process.

Absorption patterns of yellow variety including greenish yellow, yellow green and green colors, present peak of $\text{Fe}^{3+}/\text{Fe}^{3+}$ pairs at 377 and 450 nm, peak of $\text{Fe}^{2+}/\text{Ti}^{4+}$ pairs at 565 nm and also Fe^{3+} peak at 388 nm (Figures 4.16 and 4.17). These absorption peaks give clearly combination between blue and yellow that make stones appearing yellow to green colors (Figures 4.16 and 4.17). Their absorption patterns are similar to those of blue corundum samples but they show weak 565 nm peak of $\text{Fe}^{2+}/\text{Ti}^{4+}$. The sample sgb48 shows broad absorption band in range of 800-950 nm (Figure 4.16) which may be due to $\text{Fe}^{2+}/\text{Fe}^{3+}$ IVCT? while the green sample (sgb49) do not (Figure 4.17).

Colorless variety usually gives absorption patterns that are resemble to those of the yellow variety. However they mostly show lower intensities and lower absorption edges. They appear to have 377, 450 nm peaks of $\text{Fe}^{3+}/\text{Fe}^{3+}$ pairs and 388 nm peak of Fe^{3+} . These may cause vary pale yellow, but it could not be detected by naked eyes.

In conclusion, UV-VIS-NIR absorption patterns observed from Songea corundums significantly indicate causes of color of the stones. All absorption peaks in each color variety are summarized in Table 4.1, and they are compared with published data of Themelis (1992).

ศูนย์วิทยทรัพยากร
จุฬาลงกรณ์มหาวิทยาลัย

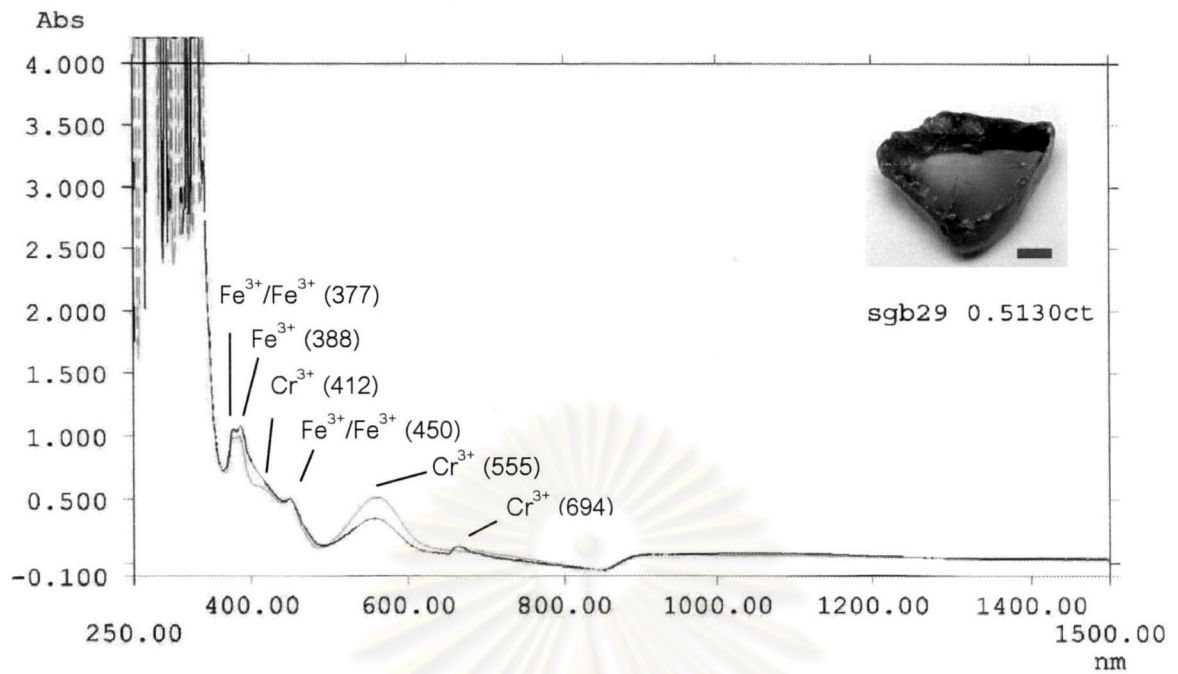


Figure 4.8 UV-VIS-NIR spectra of sample sgb29 in red variety; it shows red rim (R5/1) around orange core (O2/2).

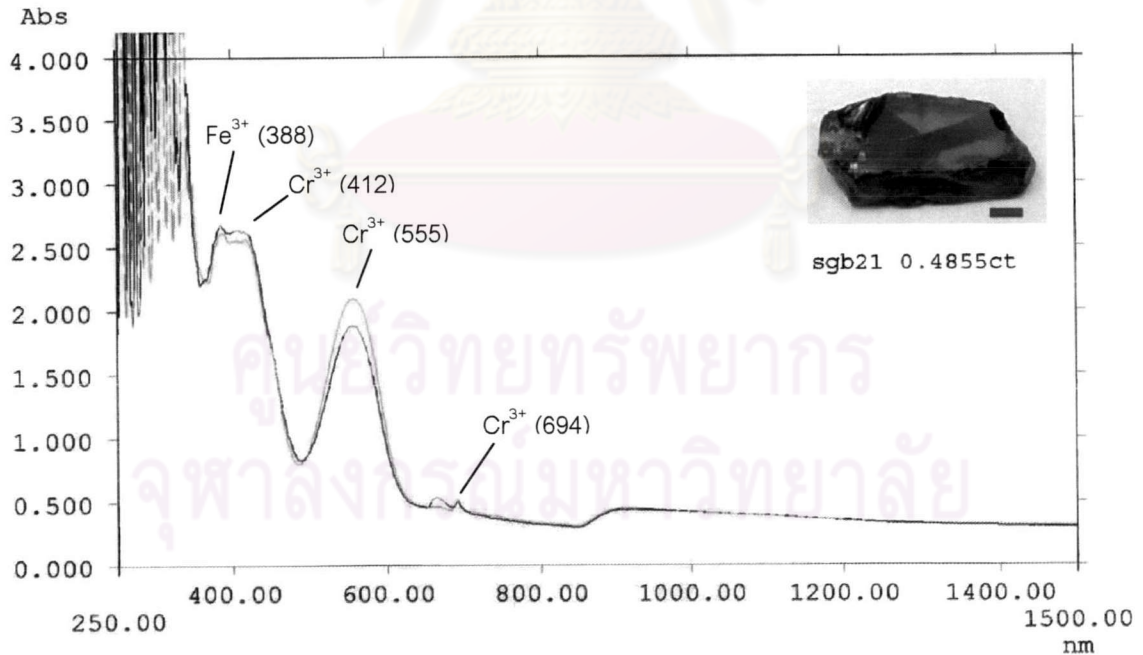


Figure 4.9 UV-VIS-NIR spectra obtained from red orange sample (sgb21) in red variety; its color code is RO/OR6/3.

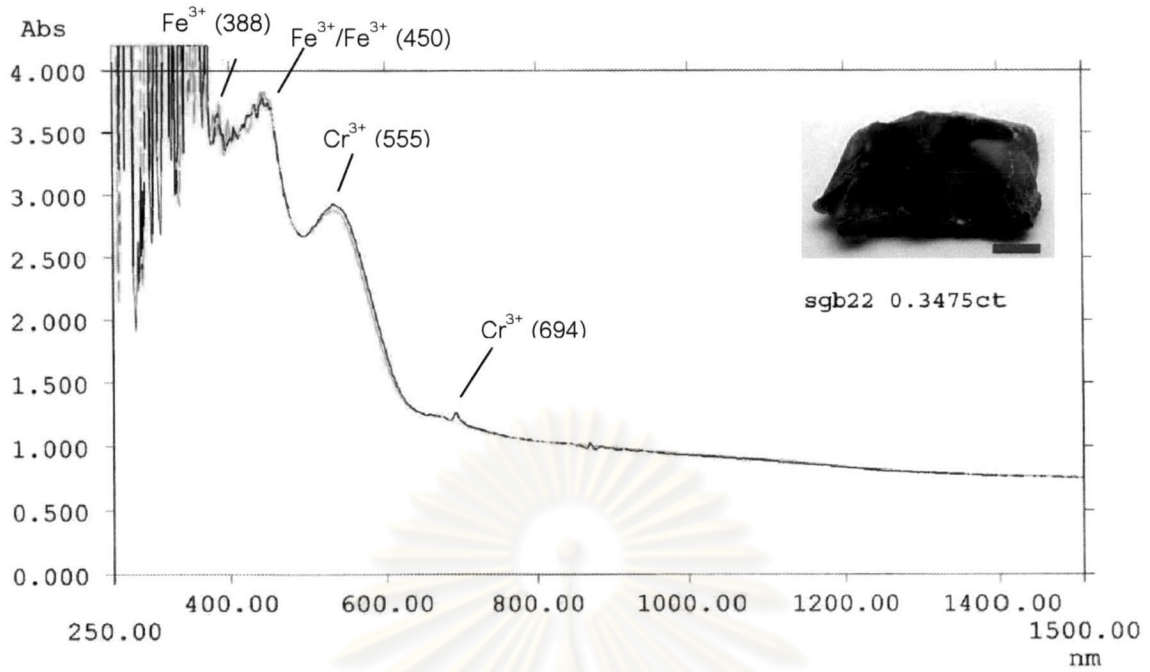


Figure 4.10 UV-VIS-NIR spectra obtained from orange sample (sgb22) in red variety; its color is code O6/3.

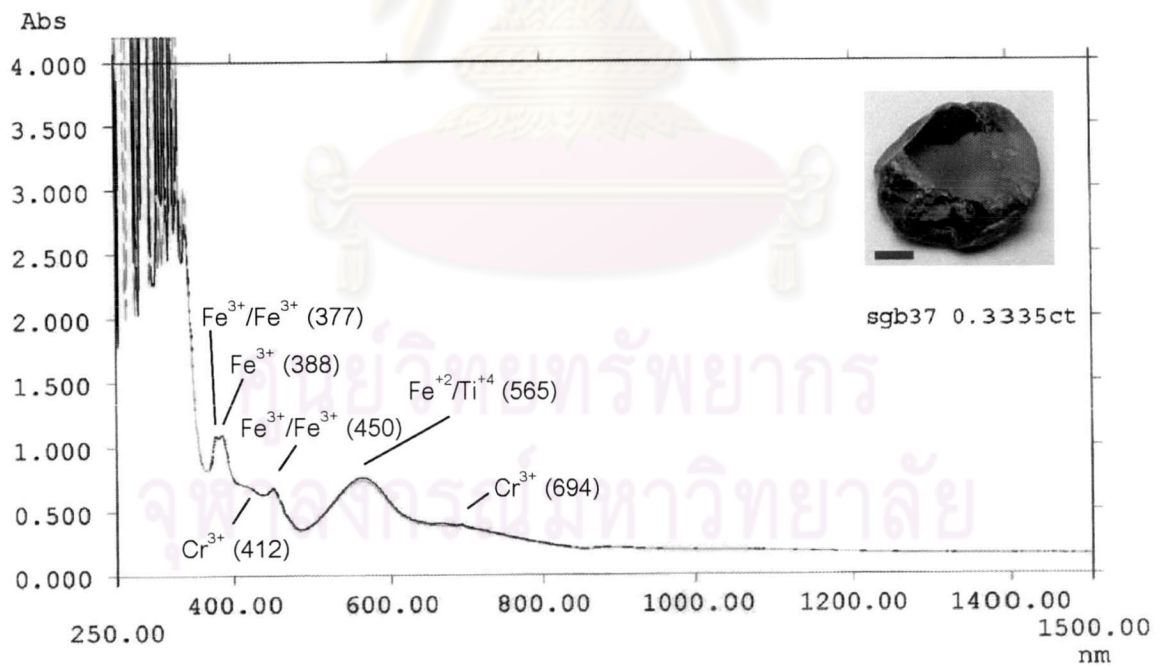


Figure 4.11 UV-VIS-NIR spectra of sample sgb37 in purple variety (color code d.rP5/3).

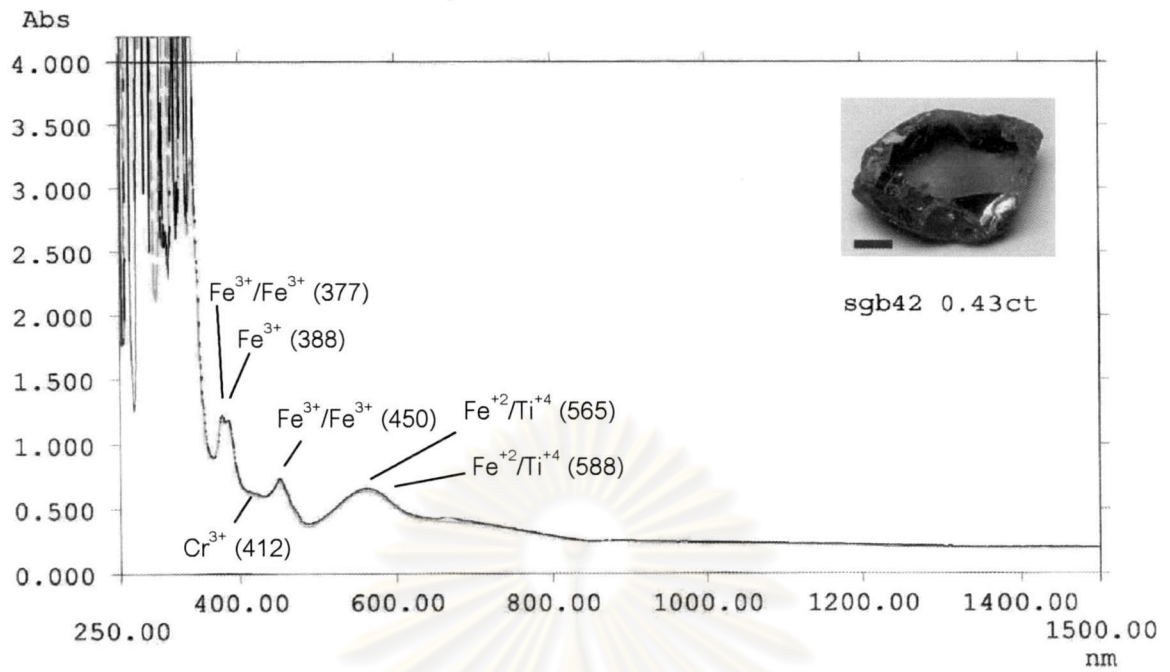


Figure 4.12 UV-VIS-NIR spectra of sample sgb42 in purple variety (color code P3/1).

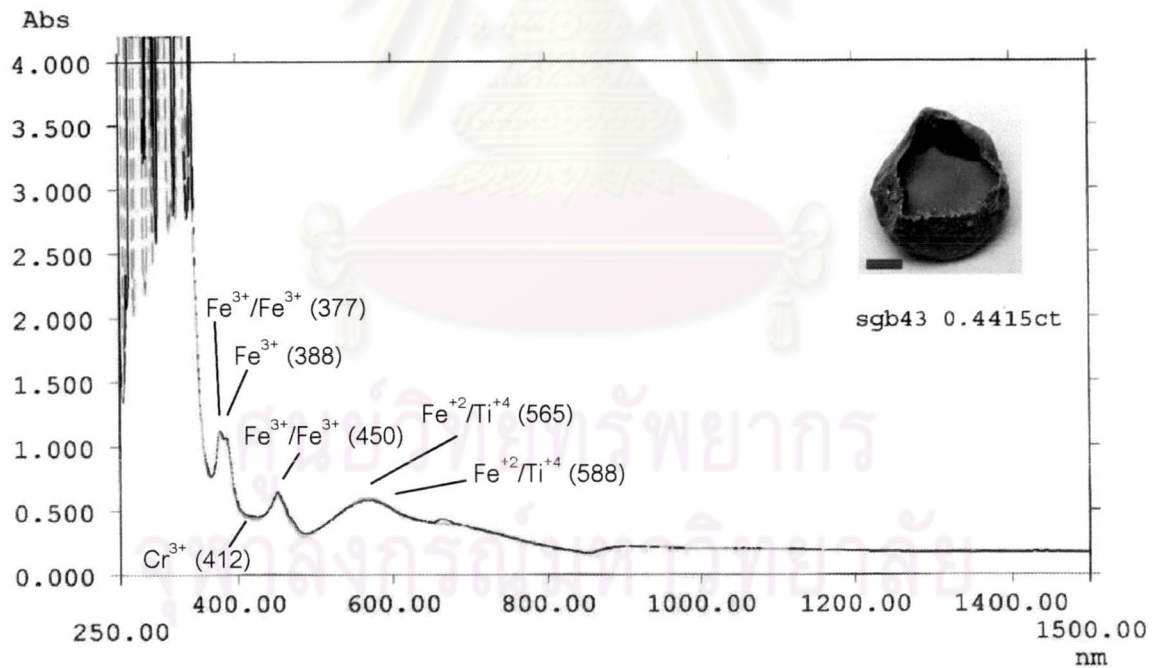


Figure 4.13 UV-VIS-NIR spectra of sample sgb43 in purple variety (color code bP6/3).

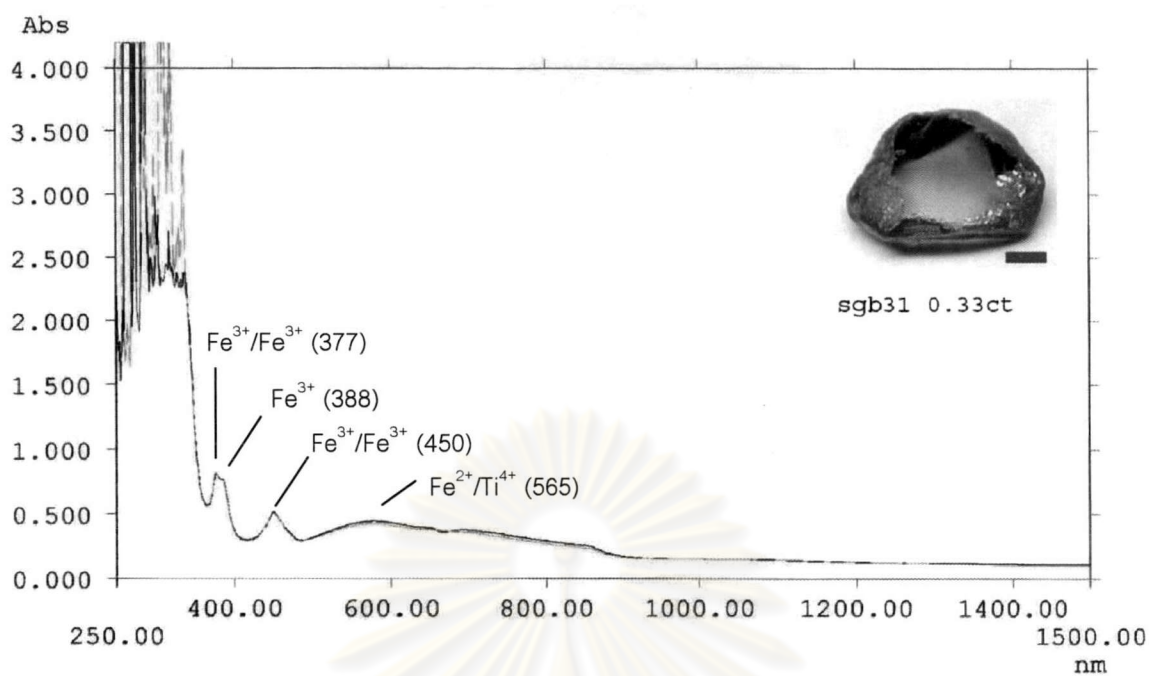


Figure 4.14 UV-VIS-NIR spectra result from sample sgb31 of blue variety; it has yellow core (YG/GY2/1) surrounded by violet blue rim (I.vB7/3).

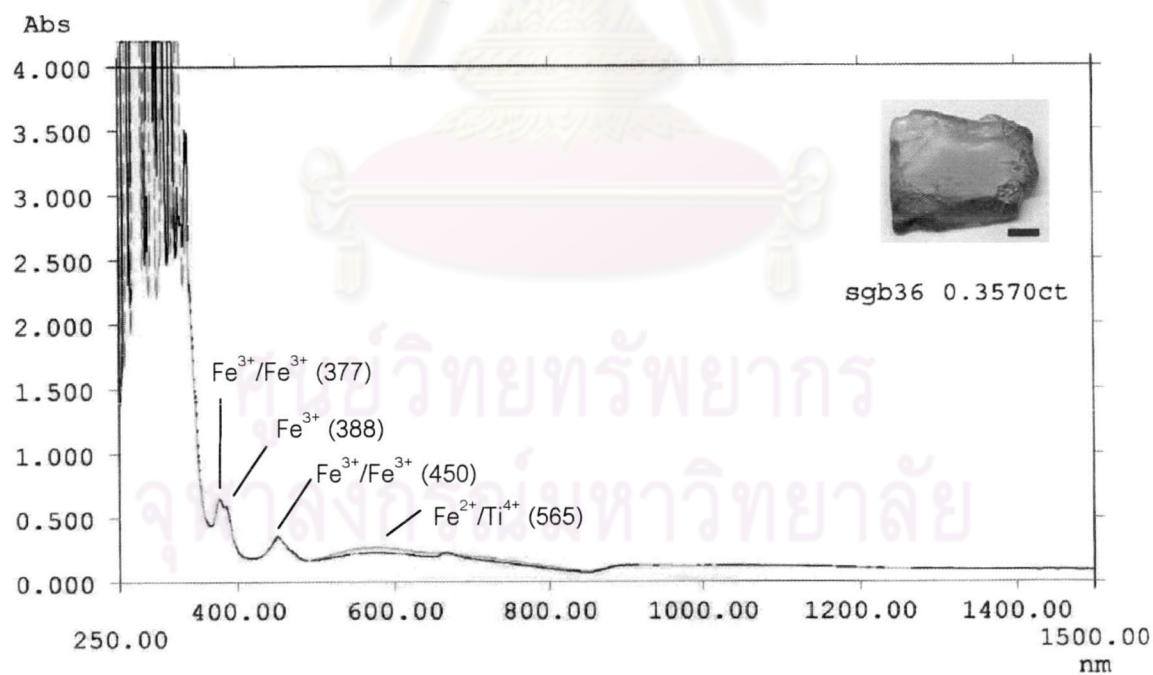


Figure 4.15 UV-VIS-NIR spectra of sample sgb36 in blue variety (color code B3/1).

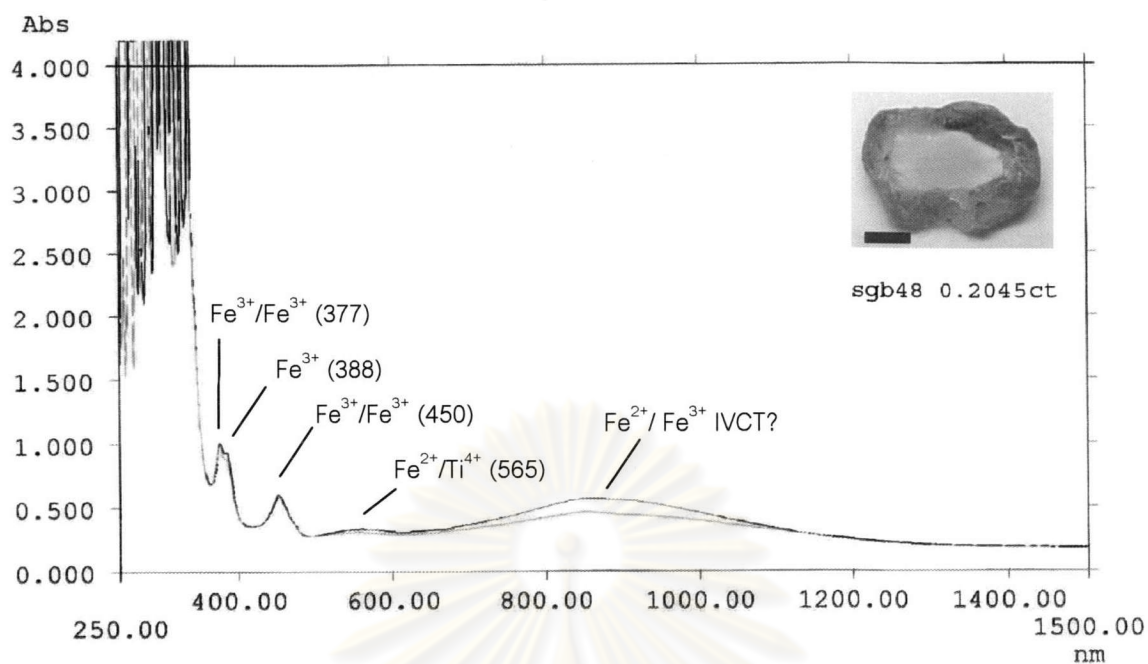


Figure 4.16 UV-VIS-NIR spectra of greenish yellow (sample sgb48) in yellow variety (color code gY2/3).

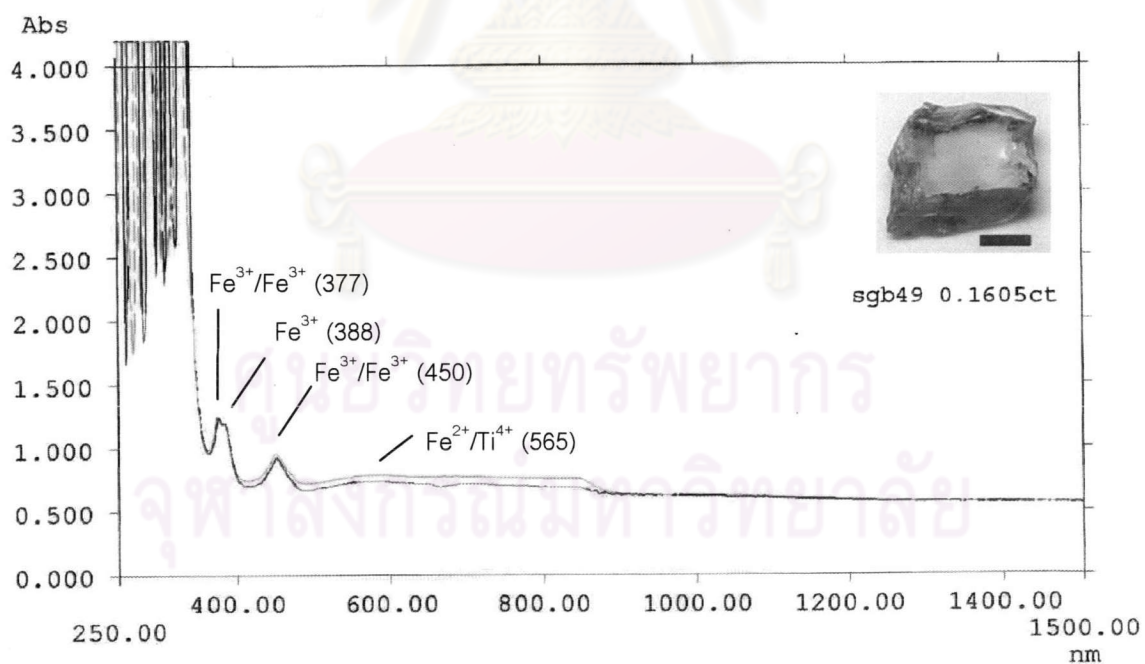


Figure 4.17 UV-VIS-NIR spectra of sample sgb49 in yellow variety (color code styG2/3).

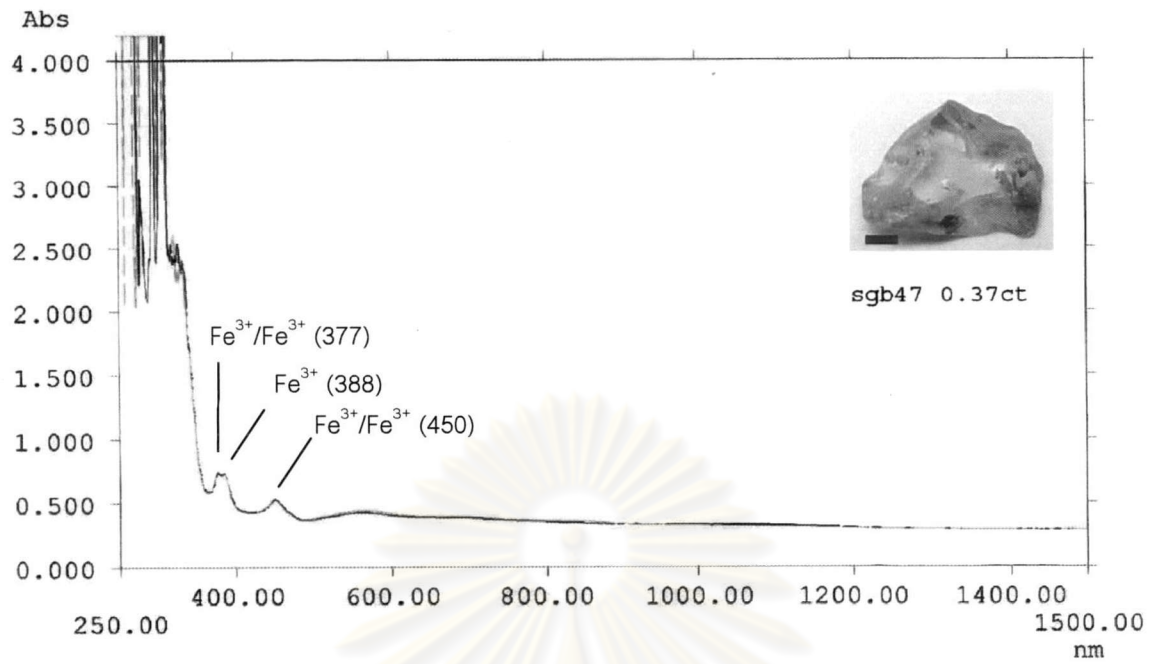


Figure 4.18 UV-VIS-NIR spectra of sample sgb47 in colorless variety (color code C(W)).

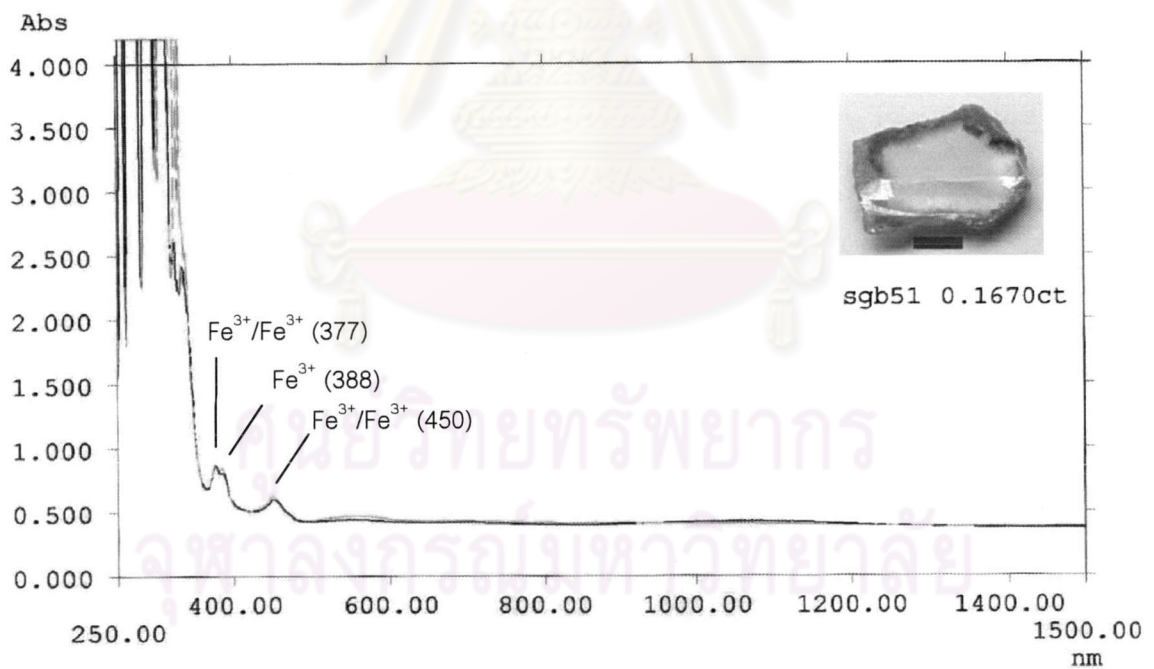


Figure 4.19 UV-VIS-NIR spectra with weak absorption peaks observed from colorless sample (sgb51).

Table 4.1 Absorption features of chromophores in Songea corundum (modified from Themelis, 1992).

| Peak (nm) | Element | Apparent Color | Color Variety of Songea corundums | | | | |
|-----------|------------------------------------|--------------------------------------------------------------|-----------------------------------|--------|------|--------|-----------|
| | | | red | purple | blue | yellow | colorless |
| 377 | Fe ³⁺ /Fe ³⁺ | blue, blue/green, green, yellow | x | x | x | x | x |
| 388 | Fe ³⁺ | pink, orange, blue, blue/green, green, yellow, golden/yellow | x | x | x | x | x |
| 412 | Cr ³⁺ | ruby; pink, blue, blue/green | x | weak | | | |
| 450 | Fe ³⁺ /Fe ³⁺ | pale orange, blue, blue/green, yellow, golden/yellow, green | x | x | x | x | x |
| 555 | Cr ³⁺ | ruby; pink, orange sapphires | x | | | | |
| 565 | Fe ²⁺ /Ti ⁴⁺ | blue, blue/green sapphires | | x | x | weak | |
| 588 | Fe ²⁺ /Ti ⁴⁺ | blue | | | x | | |
| 694 | Cr ³⁺ | ruby; pink, orange; purplish/blue | x | x | | | |

ศูนย์วิทยทรัพยากร
จุฬาลงกรณ์มหาวิทยาลัย